ARTICLE

Polydimethylsiloxane crosslinking kinetics: A systematic study on Sylgard184 comparing rheological and thermal approaches

Tiziana Bardelli ⬤ | Claudia Marano ⬤ | Francesco Briatico Vangosa ⬤

Politecnico di Milano, Dipartimento di Chimica, Materiali e Ingegneria Chimica "Giulio Natta", Milan, Italy

Correspondence
Francesco Briatico Vangosa, Politecnico di Milano, Dipartimento di Chimica, Materiali e Ingegneria Chimica "Giulio Natta", Piazza L. Da Vinci, 32, 20133 Milan, Italy.
Email: francesco.briatico@polimi.it

Abstract

In this work a systematic investigation of crosslinking kinetics of Sylgard184 polydimethylsiloxane is performed in both isothermal and dynamic conditions. The results are discussed in terms of two conversions, α_C and α_R determined by thermal and rheological analysis, respectively. Thermal analysis can well detect the first stage of the reaction, while rheological analysis starts being sensitive only at longer time. However, once the rheological response is observable, it changes with time faster than the calorimetric one. From rheology experiments it comes out that the gel point occurs at $\alpha_R = 0.53$, independently of the applied thermal history. At gel point, α_C is around 0.30 indicating that about 30% of the bonds involved in the crosslinking process is enough to create an infinite network. A modified version of the Kamal's autocatalytic model allows to fit and predict the experimental findings from both the techniques; however, two distinct sets of parameters have been used. The results of this work may be a useful tool to design appropriate curing cycles for the preparation of Sylgard184.

KEYWORDS
calorimetry, crosslinking, differential scanning calorimetry, elastomers, kinetics, rheology

1 | INTRODUCTION

Silicone rubbers, generally based on polydimethylsiloxane (PDMS), have been used in a wide range of applications for their interesting properties such as low toxicity, good biocompatibility, good physiological inertness, a high temperature and humidity stability, high transparency, and high deformability.[1] These properties allow silicon rubbers to be used in many applications such as drug delivery systems, medical devices, optical components, seals for automotive industry, electronic devices like micro electro-mechanical systems (MEMS) and flexible electronics.[2–5] The silicon rubbers that have been commonly used in these

applications are commercial polydimethylsiloxanes. PDMS is a chemically crosslinked elastomer with alternating silicon and oxygen atoms as backbone and side methyl groups. Its solidification process consists in an exothermic and irreversible polymerization and crosslinking.[1] The commercial PDMSs are usually supplied as two liquid parts kits: the components are the prepolymer and the curing agent. A thoroughly mixing of the components has to be performed before the mixture is casted or infused into a mold and the mold filling should be completed before gel point is reached in the curing process. Due to a relatively high value of the uncured mixture viscosity and to the fact that it further increases once the curing process has started,

problems in processing PDMS are commonly encountered, thus a wide characterization of the crosslinking process kinetics could provide useful information to properly design a product. One of the most used PDMS is Sylgard184 (Dow Corning). It is commonly used in soft robots manufacturing or for the production of biomedical soft tissues, elastic lenses, and waveguides[6–14] that would benefit of a deeper knowledge of the crosslinking kinetics of their soft components. The crosslinking reaction of Sylgard184 takes place spontaneously at room temperature over approximately 48 h, but this time can be shortened by heating.[15] The thermal history applied may affect PDMS properties, such as its strength and stiffness as well its refractive index and thus affecting the performance of the final PDMS based product.

The evolution of the polymer crosslinking can be monitored following the change in some of the material physical properties induced by the occurring chemical reaction.[16] As reported in literature, many researchers have developed kinetic models based on the evaluation of the heat of reaction obtained from thermal analysis.[17–21] Others have monitored the evolution of the crosslinked structure through its effects on mechanical properties.[20,22] To our knowledge, only Harkous et al[20] compared the outcomes of both these approaches, but they proposed a kinetic model interpreting only the results of the thermal analysis.

In this study, the change with time of both the heat of reaction related to the crosslinking process and of the dynamic modulus of the resulting material, determined by calorimetric and rheological analysis respectively, was evaluated to investigate the crosslinking process kinetics of the Dow Corning PDMS Sylgar184 and the results have been interpreted on the basis of a theoretical model. To the authors knowledge, a kinetic model has not yet been reported in literature for this material. The two quantities have been measured under several temperature histories: two different definitions for conversion, based on thermal and mechanical responses respectively, have been introduced. In both cases a modified version of the Kamal's autocatalytic model[23] has been used to model the time dependency of conversion. The effects of the thermal history on the final properties of the PDMS is currently under investigation and will be widely discussed in a separate work.

2 | EXPERIMENTAL

2.1 | Materials

The PDMS Sylgard184, provided by Dow Corning, is a two components system consisting of an elastomer base (component A), with a viscosity of 5100 mPa s and a curing agent (component B). Both the components are liquid and transparent. Typically, the elastomer base contains linear PDMS pre-polymers with two vinyl end groups that react with the component B multifunctional crosslinker leading to a three-dimensional crosslinked network. The hydrosilylation reaction mechanism of the PDMS is known and reported in literature.[24,25]

The exact composition of Sylgard184 is proprietary, anyway, the materials safety data sheet states that the elastomer base (component A) contains mainly *dimethyl siloxane, dimethylvinylsiloxy-terminated (CASRN: 68083–19-2)* and *dimethylvinylated and trimethylated silica (CASRN: 68988–89-6)* and the curing agent (component B) contains mainly *siloxanes* and *silicones, dimethyl, methylhydrogen (CASRN: 68037–59-2), dimethyl siloxane, dimethylvinylsiloxy-terminated (CASRN: 68083–19-2), dimethylvinylated* and *trimethylated silica (CASRN: 68988–89-6)* and *methyl-vinylcyclosiloxane (CASRN: 2554-06-5).*

2.2 | PDMS preparation

The two components were mixed, at room temperature, with a low speed helix mixer (200 rpm speed, helix diameter 20 mm, beaker diameter 30 mm) for 10 min, in 10 : 1 (A : B) mass ratio, as suggested by the supplier.[15] The viscosity of the mixture immediately after the mixing of the two components was measured and resulted equal to 3900 mPa s. The mixture was first degassed in a vacuum bell jar for 20 min (low vacuum $P = 9 \cdot 10^4$ Pa) in order to remove air bubbles incorporated during mixing and then kept at 4 °C and used for testing within 5 h from mixing. It was verified that there were no differences among the material properties when measured in this time lag: the variation of the rheological response in the early stage of the test was within the experimental error and the repeatability of the measurements further confirms the stability of the materials in this time lag.

2.3 | Thermal histories

In both the crosslinking reaction analyses two types of thermal histories were considered (Figure 1):

- thermal histories in dynamic conditions (hereinafter referred to as DINT): the sample was kept 1 min at 25 °C, then it was heated up to 130 °C at constant rate. Four different rates were adopted: 1, 2, 4, 8 °C min⁻¹. In these histories the crosslinking is expected to occur during heating (dynamic conditions).
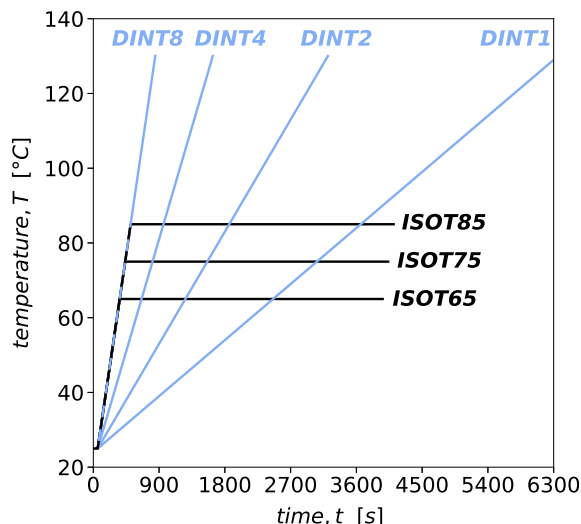
FIGURE 1 Thermal histories imposed to the material in both calorimetric and rheological analyses (temperature vs. time). In black "isothermal conditions", in blue "dynamic conditions" [Color figure can be viewed at wileyonlinelibrary.com]

- thermal histories in isothermal conditions (hereinafter referred to as ISOT): the sample was kept for 1 min at 25°C, then it was heated at the rate of $8\,°C\,min^{-1}$ to the curing temperature T_c at which it was kept for 1 h. Three different curing temperatures were considered: 65, 75, 85°C. In these histories the crosslinking is expected to occur, during the isothermal step, at the constant curing temperature (isothermal conditions).

The thermal stability of Sylgard184 in the explored temperature range is well documented. The technical datasheet states that its temperature of application range is from−45 to 200°C [15] and Liu et al[26] experimentally verified that thermal decomposition of Sylgard184 starts at temperature about 200°C and reaches its maximum rate at 310°C.

2.4 | Differential scanning calorimetry

Differential scanning calorimetry (DSC) measurements were performed under nitrogen, at atmospheric pressure, using a Mettler Toledo DSC 3 calorimeter. The sample mass used ranged from 16 to 29 mg. Different thermal histories were applied, as detailed in section 2.3. Each test was carried out twice to verify the repeatability of the obtained values.

Since hydrosilylation reaction is an exothermic process,[27] the heat released in time $Q(t)$, detected as heat flow $dQ(t)/dt$ with DSC analysis, can be used to describe the progress of the crosslinking process.

A conversion rate $d\alpha_C/dt$ can be defined as follows:

$$\frac{d\alpha_C}{dt} = \frac{1}{Q_T}\frac{dQ(t)}{dt} \tag{1}$$

where Q_T is the total heat of the reaction, obtained integrating the exothermic peak on the total reaction time.

The conversion $\alpha_C(t)$ can be obtained integrating the reaction heat curve at each time step and normalizing over the total heat Q_T:

$$\alpha_C(t) = \frac{\int_0^t \left(\frac{dQ(t)}{dt}\right)dt}{\int_0^{t_{end}} \left(\frac{dQ(t)}{dt}\right)dt} = \frac{Q(t)}{Q_T} \tag{2}$$

where t_{end} represents the time at which the reaction is completed.

If it is assumed that, during the crosslinking reaction, the formation of each covalent bond releases the same amount of energy, the conversion can be related to the amount of bonds formed within the network.[28,29]

2.5 | Rheometry

Rheological measurements were performed using an Antor Paar MCR 502 rheometer in oscillatory mode, using parallel plates (diameter 25 mm). The PDMS mixture was first poured on the rheometer lower plate, then the upper plate was moved toward the lower one and positioned at a distance of 1 mm and the material in excess was trimmed before starting the test. Measurements were performed in air and at atmospheric pressure. The rheometer is equipped with a Peltier plate and a hood to control the testing temperature. A normal force of 1 N was imposed during the test to ensure no slip between the plates and the sample. Each measurement was carried out at least three times to verify the repeatability of the obtained values.

The measurements were carried out at the constant frequency of 1 Hz. Given the wide variation of the complex modulus, the strain amplitude was set to 5% for a complex modulus up to $4\cdot10^5$ Pa and to 0.5% for larger values. In both cases the linearity of the measured properties was verified. The thermal histories applied are the same of the thermal analysis and are reported in section 2.3.

In order to describe the crosslinking kinetics, the time dependence of the storage modulus (G') during curing, was considered. Among the definition found in literature,[20,30] the conversion $\alpha_R(t)$, defined as follows, was adopted:

$$\alpha_R(t) = \frac{\ln G'(t) - \ln G'_{min}}{\ln G'_{max} - \ln G'_{min}} \tag{3}$$

where G'_{min} and G'_{max} are respectively the minimum and the maximum value of the storage modulus during curing.

The conversion rate is the first derivative of $\alpha_R(t)$ in time: $d\alpha_R/dt$.

A "logarithmic definition" was chosen as it allows to better observe the trend of the mechanical property considered, given the wide variation expected for G' ranging from $G' \approx 10^{-4}$ Pa when the reaction starts (liquid state) to $G' \approx 10^6$ Pa at the end of the reaction (solid state). Furthermore, this description emphasizes the liquid solid transition that is a very important step in all crosslinking processes.

3 | CROSSLINKING KINETIC MODELING

The conversion rates $d\alpha/dt$ determined from both the reaction kinetics analyses performed, were assumed to be a function of T and α separately. To describe the rate dependence on these two variables, a modified version of the autocatalytic model proposed by Kamal et al,[23] often used for silicon rubbers[17–20] was adopted:

$$\frac{d\alpha}{dt} = (K_1 + K_2 \, \alpha^m)(1-\alpha)^n \tag{4}$$

where m and n are the orders of the reaction and K_1 and K_2 are rate constants defined by Arrhenius equation:

$$K_2 = A_2 \, exp\left(-\frac{E_2}{RT}\right) \tag{5}$$

with R=gas constant, T= absolute temperature, A_{1-2}= pre-exponential factor, E_{1-2}= activation energy.

Since an order of the reaction higher than 2 is extremely uncommon, it is assumed $m+n=2$.[18,30]

Assuming, then, $E_1 = E_2 = E$ the model can be reduced to an equation of the form:

$$\frac{d\alpha}{dt} = k(T)f(\alpha) \tag{6}$$

where:

$$k(T) = exp\left(-\frac{E}{RT}\right) \tag{7}$$

$$f(\alpha) = \left(A_1 + A_2 \, \alpha^{(2-n)}\right)(1-\alpha)^n \tag{8}$$

The model so defined has 4 parameters (E, A_1, A_2, n) to be identified in order to fully describe the kinetics.

Two different sets of kinetic model parameters (E, A_1, A_2, n) were separately obtained, respectively for the conversions α_R and α_C differently evaluated, by minimization of the function D:

$$D = \sum_{i=1}^{w} \frac{\sqrt{\sum\left(\left|\frac{d\alpha}{dt}\right|_{exp} - \left|\frac{d\alpha}{dt}\right|_{model}\right)^2_i}}{w} \tag{9}$$

over the w experimental curves obtained from all the thermal histories performed.

To obtain the evolution of α_R and α_C in time, the model was then numerically integrated with Runge Kutta 4th order method. All the calculations were performed using Matlab2018.

For the integration, mathematical functions describing the whole thermal histories actually applied must be defined. In other words, they must also consider the initial heating ramp of the isothermal histories (ISOT) and the initial isothermal step at 25 °C of the dynamic thermal histories (DINT). In particular, for DINT experiments the following ramp function was used:

$T(t) = \dot{T} \frac{t-a+|t-a|}{2} + b$ with $0 \le t \le 4600$ s

where b is the initial temperature, a is the time during which the initial temperature is kept constant and $\dot{T}$ is the heating rate. In this work $b = 25$ °C, $a = 60$ s, $\dot{T} = 1, 2, 4, 8$ °C min^{-1}.

For ISOT experiments the following ramp function was used:

$T(t) = \dot{T} \frac{t-c-|t-c|}{2} + T_c$ with $60 \le t \le 4600$ s

where T_c is the curing temperature, c is the time to reach T_c and $\dot{T}$ is the heating rate used to reach T_c. In this work $c = 370$ s, 445 s, 515 s for, respectively, $T_c = 65$ °C, 75 °C, 85 °C, and $\dot{T} = 8$ °C min^{-1}.

Neglecting the initial time required to heat the sample up to the curing temperature T_c in isothermal conditions would have led to significant errors in α prediction.

The experimental curves obtained from the thermal histories ISOT65, ISOT75, ISOT85, DINT1, DINT2, DINT4 were taken into consideration for model parameters identification, while experimental curves from DINT8 were used to verify the prediction ability of the model.

Equation (6) describes the rate of a single-step process (one single activation energy, E). Although Equation (6) is widely used in the majority of the kinetic methods in the area of crosslinking reactions,[16] Friedman

isoconversional method was used to verify that the single-step kinetic assumption was a reasonable approximation for the more complex reaction process under study.[16]

The method allows to check the dependency of E on α. Considering that the conversion rate $d\alpha/dt$ at a fixed value of conversion α^*, for the ith thermal history, is only a function of temperature, the following equation can be derived from Equation (6):

$$ln\left(\frac{d\alpha}{dt}\right)_{\alpha^*,i} = ln[f(\alpha)] - \frac{E_{\alpha^*}}{RT_{\alpha^*,i}} \tag{10}$$

$T_{\alpha^*,i}$ indicates the temperature at which the conversion α^* is reached under the ith thermal history applied. Thus, at a given α^*, E_{α^*} can be calculated from the slope of
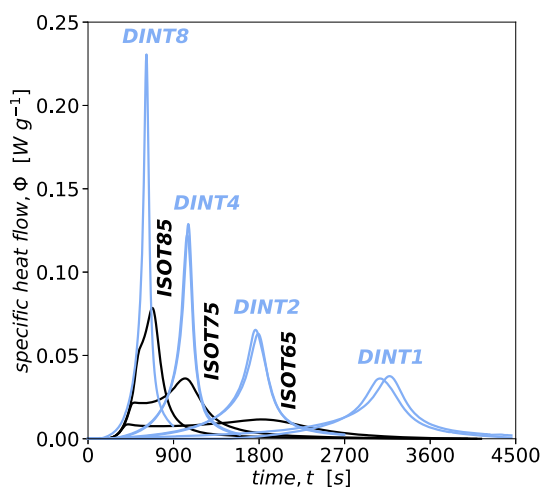
$ln(d\alpha/dt)_{\alpha^*,i}$ versus $1/T_{\alpha^*,i}$ plot. The index i denotes the temperature program.

In this work, α was varied from 0.05 to 0.90 with a step of 0.05, as recommended by Vyazovkin et al.[16]

# 4 | RESULTS AND DISCUSSION

4.1 | Experimental data

Results from calorimetry and from rheometry are shown in Figure 2 and Figure 3, respectively. Results from calorimetry (Figure 2) show that the heat flow arrives to its peak point with a rate that depends on the applied thermal history: by increasing the heating rate (from DINT1 curve to DINT8 curve) or the isothermal curing temperature (from ISOT65 curve to ISOT85 curve), the peak point increases in intensity and occurs at shorter time.

The overlap of the first part of the ISOT curves with the DINT8 one is consistent with the fact that in ISOT conditions the initial heating ramp applied to reach the curing temperature T_c is carried out at $8\,°C\,min^{-1}$, that is the same rate adopted in the DINT8 thermal history (see Figure 1).

Results from rheometry (Figure 3) show that after an induction time, G' increases sharply; then the rate of G' variation decreases, and the modulus tends to a plateau.

Generally speaking, the initial increment of the modulus indicates the growth of the polymer chains, due to the hydrosilylation reaction, up to the formation of a three-dimensional network. The moment at which this network is formed is called "gel point". After this point, further crosslinks gradually form, until the network is completed.[31] During the production of the material, the insight regarding the gel point is crucial since it reflects the change in the mechanical behavior of the material, from liquid-like to solid-like.

FIGURE 2 Specific heat flow vs. time for different thermal histories. In black "isothermal conditions", in blue "dynamic conditions". Raw data were corrected by baseline subtraction [Color figure can be viewed at wileyonlinelibrary.com]

FIGURE 3 Mean storage modulus, G' (continuous lines) and mean loss modulus, G'' (dashed lines) with the respective error bands, versus time in (a) "dynamic conditions" and (b) "isothermal conditions". The diamonds indicate the gel points [Color figure can be viewed at wileyonlinelibrary.com]
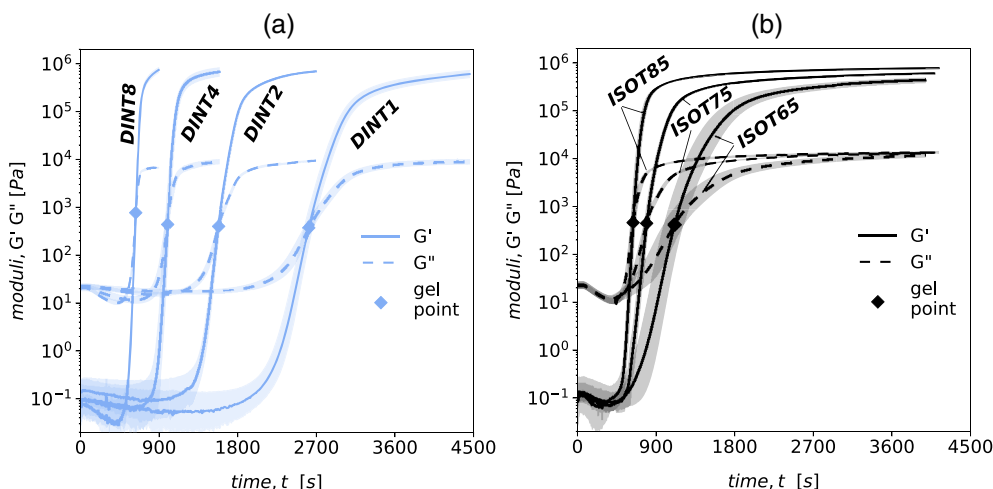
Different methods for determining the gel point are reported in literature.[20,27,32–35] In this study, as a first approximation, the point at which the storage modulus equals the loss modulus ($G' = G''$) was considered as the gel point (diamonds in Figure 3). This simple method was also used, on another PDMS, by Harkous et al[20] in their study in which they show that the estimation of the gel point as the point in which $G' = G''$ leads to results similar to those of different more accurate analyses.

Table 1 shows the time at which the gel point occurs for the different thermal histories in this study, with their relevant standard deviations.

The time at which gel point occurs is longer the lower the heating rate or the isothermal curing temperature is. In particular, it can be observed that the time at the gel point doubles if the isothermal curing temperature decreases from 85 to 65 °C and it quadruples if the heating rate is reduced from 8 to 1 °C min^{-1}: a variation of the curing temperature of only 20 °C or a change in the heating rate lower than one order of magnitude, considerably affects the gel point time, and this highlights how these issues should be considered to optimize the curing process of the material.

TABLE 1   Gel point time for the different thermal histories

Thermal history	Time at gel point [s]
DINT1	2609 ± 50
DINT2	1583 ± 19
DINT4	995 ± 30
DINT8	635 ± 10
ISOT65	1099 ± 110
ISOT75	791 ± 27
ISOT85	638 ± 24

The conversion α_C and the conversion rate $d\alpha_C/dt$ were determined according to Equation (2) and (1) from calorimetric analysis. The conversion α_R and the conversion rate $d\alpha_R/dt$, were calculated from rheological analysis with Equation (3) and its numerical derivative. The results of data elaborations are shown in Figure 4 and Figure 5, respectively.

It can be seen that α_C slowly increases almost since the beginning of the experiment while α_R starts to grow only after an induction time (this is more visible for the DINT histories). This means that, at the beginning of the process of PDMS network formation, chemical bonds form releasing heat, without inducing any change in the material mechanical properties. Despite this, after the induction period, α_R increases faster than α_C and the maximum of the conversion rate $d\alpha/dt$ occurs always at shorter time in rheological analysis than in calorimetric analysis. This difference is more evident at low heating rate, for tests in "dynamic conditions" and at low curing temperature for tests in "isothermal conditions".

It can also be noticed that, for the same i^{th} thermal history applied in DINT experiments, the maximum conversion rate is the same for both the calorimetric and rheological measurements ($\max d\alpha_{C,i}/dt = \max d\alpha_{R,i}/dt$), while in the ISOT tests the maximum conversion rate is higher for the rheological measurements ($\max d\alpha_{C,i}/dt < \max d\alpha_{R,i}/dt$).

Finally, the gel point (diamonds in Figure 4 and Figure 5) occurs always shortly after the time of the maximum of the rheological conversion rate $d\alpha_R/dt$ and, at that time, the conversion for the rheological tests is $\alpha_R = 0.53 \pm 0.01$ while, the conversion measured from calorimetric tests is lower and equal to $\alpha_C = 0.30 \pm 0.05$. This indicates that whatever is the time at which the liquid like−solid like transition (the gel point) takes place, which depends on the reaction kinetics and thus on the applied thermal history, the conversion at the gel point is
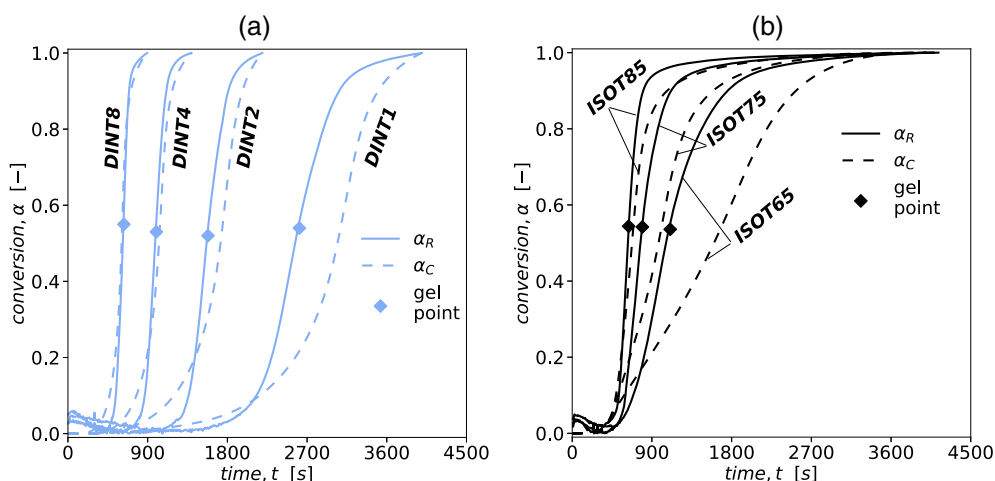

FIGURE 4 Comparison of conversion from calorimetric analysis α_C (dashed lines) and conversion from rheological analysis α_R (continuous lines) vs. time in (a) "dynamic conditions" and (b) "isothermal conditions" [Color figure can be viewed at wileyonlinelibrary.com]

FIGURE 5 Comparison of conversion rate from calorimetric analysis dα_C/dt (dashed lines) and conversion rate from rheological analysis dα_R/dt (continuous lines) versus time in (a) "dynamic conditions" and (b) "isothermal conditions". The diamonds indicate the gel points [Color figure can be viewed at wileyonlinelibrary.com]
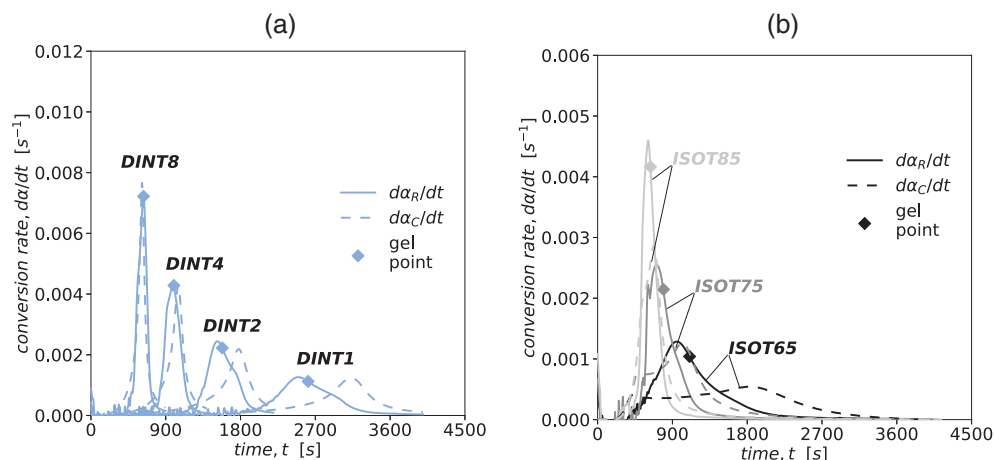
FIGURE 6 Activation energy vs. conversion calculated according to Friedman isoconversional method. (a) Calorimetric measurements: Empty dots refer to the conversion range in which the diffusion mechanism is relevant. (b) Rheological measurements [Color figure can be viewed at wileyonlinelibrary.com]
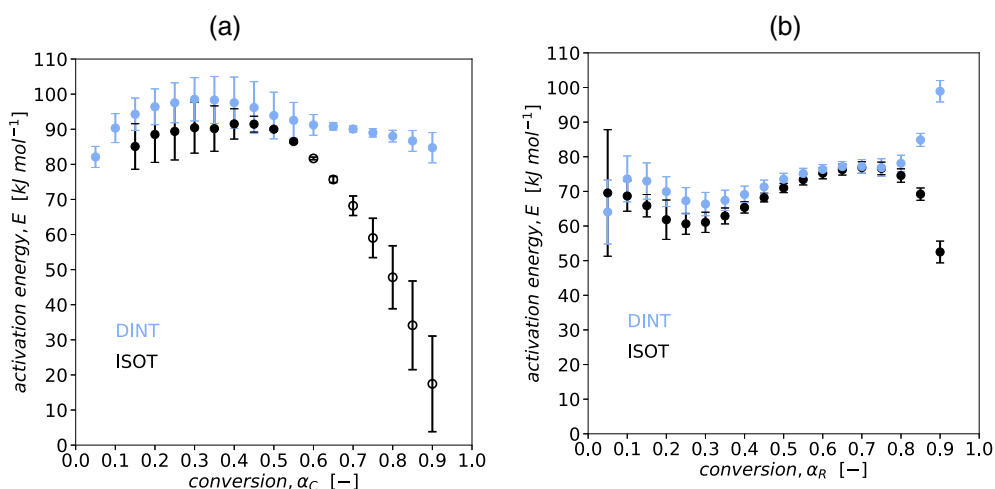
the same. Furthermore, as mentioned in section 2.4, since the conversion from calorimetric observations can be related to the amount of bonds formed for the network production,[28] the value of α_C at the gel point indicates that only about 30% of the chemical bonds formed during the whole crosslinking process are involved in the production of the gel point infinite network; the material is already in a gel state at a quite early stage of the chemical reaction and the further bonds formation is just responsible for the structure of the final network on which the mechanical properties will depend.

4.2 | Kinetic models

The activation energy E, calculated according to Friedman isoconversional method described in Section 3, is plotted versus the conversion α in Figure 6 for calorimetric (a) and rheological (b) measurements, respectively.

For calorimetric analysis, the activation energy E can be considered fairly constant, within the experimental data dispersion, up to a conversion α_C of 0.55, with a mean value of 93 ± 4 kJ mol^{-1}. This value falls in the range reported in literature for different PDMS.[18,20]

After $\alpha_C = 0.55$ the activation energy remains constant in DINT curves, while in ISOT it decreases significantly. This suggests that a diffusion controlled mechanism starts to be relevant in isothermal curing.[16,36]

E changes observable at high values of conversion are consistent with other studies[16,37,38] and can be associated with the change in the mobility of the molecules during the crosslinking process. As shown at the end of section 4.1, at the gel point α_C is about 0.30, thus $\alpha_C = 0.55$ corresponds to an already partially crosslinked system in which the mobility is limited. This limitation affects the reaction mechanism in ISOT, while in DINT the increase in temperature partially compensates the decrease in the mobility due to crosslinking.

For rheological analysis (Figure 6(b)), the activation energy E remains constant, within the experimental data dispersion, up to a conversion α_R of 0.8, with a mean value of 71 ± 5 kJ mol^{-1}.

A single step kinetics is confirmed for all the conditions except ISOT experiments in which it is confirmed only for the first part of the reaction. Thus, the Kamal's autocatalytic model, often used for silicon rubbers,[17–20] was assumed as a reasonable approximation for the reaction in this study.

The Kamal's model parameters (E, A_1, A_2, n) were determined in two steps, separately for thermal and rheological analysis, using the least squares criterium described in Section 3.

For calorimetric analysis, data in the range $0.15 \leq \alpha_C \leq 0.55$ (in which the Friedman analysis indicated constant activation energy) were first used to determine all the model parameters. Then, a new estimation of the parameter n alone was obtained by using the data in the whole range $0 \leq \alpha_C \leq 1$, maintaining constant the other 3 parameters. The parameters obtained are the following: $E = 93.5$ kJ mol^{-1}, $A_1 = 7.2 \cdot 10^{10}$ s^{-1}, $A_2 = 2.9 \cdot 10^{11}$ s^{-1}, $n = 0.96$.

For rheological analysis, first data in the range $0.10 \leq \alpha_R \leq 0.80$ (constant activation energy) were used to determine all the parameters, then a better estimation of n was obtained considering only the first part of the curves $0 \leq \alpha_R \leq \alpha_{Rl}$ where α_{Rl} is the value corresponding to the maximum of $d\alpha_R/dt$. The parameters obtained are the following: $E = 71.5$ kJ mol^{-1}, $A_1 = 0$ s^{-1}, $A_2 = 4.8 \cdot 10^8$ s^{-1}, $n = 1.28$.

The values of the activation energy E are in good agreement with the above reported values obtained with Friedman isoconversional method. The value of A_1 is related to the trend of the initial conversion rate: the A_1 value different from zero obtained in DSC experiments, describes the initial slow release of heat, while, for rheological curves, $A_1 = 0$ is associated to the initial induction time of the phenomenon.

Table 2 collects these parameters values and, for comparison, also reports the parameters values of kinetic models (detailed in Table 3) used by Harkous et al,[20] Hong and Lee[18] and Zhang et al[19] for different silicon rubbers. It is worth to highlight that, to the authors knowledge, this is the only work in which the crosslinking kinetics modeling has been performed both on data from calorimetric measurements and on data from rheological measurements: this has allowed to match the information obtained from these two independent techniques. For example, it was observed that heat release can be detected without the material has changed its mechanical behavior and it is expected that this result could be thought to be valid for any other PDMS.

Figure 7 and Figure 8 show the comparison between experimental (continuous lines) and calculated (dashed lines) conversion rates $d\alpha/dt$ for calorimetric analysis and rheological analysis, respectively.

For calorimetric DINT experiments (Figure 7(a)), there is quite a good agreement between the experimental and the predicted data, for all the thermal histories, even though experimental peak values are higher than the calculated ones. For calorimetric ISOT experiments

TABLE 2 Values of kinetic model parameters for PDMS crosslinking process derived from calorimetric and rheological analyses performed in this study. Data from literature are reported for comparison

Authors method PDMS used	Model Code [a]	Model parameters					
		E_1 kJ mol^{-1}	E_2 kJ mol^{-1}	A_1 s^{-1}	A_2 s^{-1}	$m-$	$n-$
This study Calorimetric analysis Sylgard184	-ACM1-	93.5	93.5 [b]	$7.2 \cdot 10^{10}$	$2.9 \cdot 10^{11}$	1.04 [c]	0.96
This study Rheological analysis Sylgard184	-ACM1-	71.5	71.5 [b]	0	$4.8 \cdot 10^8$	0.72 [c]	1.28
Harkous et al.[20] Calorimetric analysis Silbione LSR4350 HC	-ACM2-	73.6	73.6	$2.11 \cdot 10^7$	$6.97 \cdot 10^8$	1.31	1
Hong and Lee[18] Calorimetric analysis Silbione LSR 4330	-ACM3-	—	116	—	$1.12 \cdot 10^{15}$	1.178c	0.822
	-NthOM-	109	—	$1.02 \cdot 10^{13}$	—	—	2
Zhang et al.[19] Calorimetric analysis LTV silicone rubber	-NthOM-	553.87	—	$9.29 \cdot 10^{70}$	—	—	1.28

[a]See Table 2 for the meaning of the CODE.

[b]By assumption $=E_1$.

[c]By assumption $=2-n$.

(Figure 7(b)), even though the peak time and intensity dependency on curing temperature is properly predicted by the model (the lower the temperature the longer the

TABLE 3 Models reported in literature for the prediction of PDMS kinetics

Model CODE	Model	Assumptions
ACM1 (modified autocatalytic model)	$\frac{d\alpha}{dt} = (K_1 + K_2\,\alpha^m)(1-\alpha)^n$ $K_{1-2} = A_{1-2}\,exp\left(-\frac{E_{1-2}}{RT}\right)$	$E_1 = E_2 = E$ $m = 2 - n$
ACM2 (modified autocatalytic model)	$\frac{d\alpha}{dt} = (K_1 + K_2\,\alpha^m)(1-\alpha)^n$ $K_{1-2} = A_{1-2}\,exp\left(-\frac{E_{1-2}}{RT}\right)$	
ACM3 (modified autocatalytic model)	$\frac{d\alpha}{dt} = K\,\alpha^m(1-\alpha)^n$ $K = A\,exp\left(-\frac{E}{RT}\right)$	$m = 2 - n$
NthOM (nth order model)	$\frac{d\alpha}{dt} = K\,(1-\alpha)^n$ $K = A\,exp\left(-\frac{E}{RT}\right)$	

peak time and the lower the intensity), larger differences between the experimental and the predicted curves can be observed. On the other hand, the model adopted refers to a single-step kinetics (one single activation energy, E) which is a hypothesis not fully verified in this case.
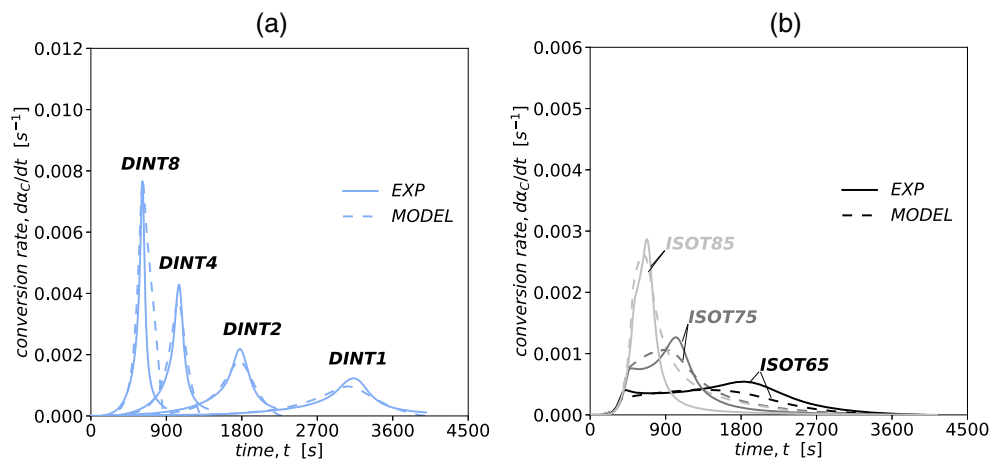
In rheological analysis (Figure 8), the comparison between the experimental and the predicted data reveals a very good agreement for all the thermal histories. As concerns the DINT8 experiment, the predicted peak is higher than the experimental one. This may be due to the fact that at such high heating rate the sample temperature is not homogeneous: during heating, the temperature in the core of the sample is lower than the programmed one, thus the actual process will be slower than the prediction made assuming a homogeneous heating of the whole sample.

Despite the differences observed in Figure 7, by integrating Kamal's model, an accurate description of α_C conversion during time was obtained, as shown in Figure 9, for all the thermal histories except ISOT65. Regarding the α_R dependence on time (Figure 10) also in this case the model prediction is very good for all the experiments.
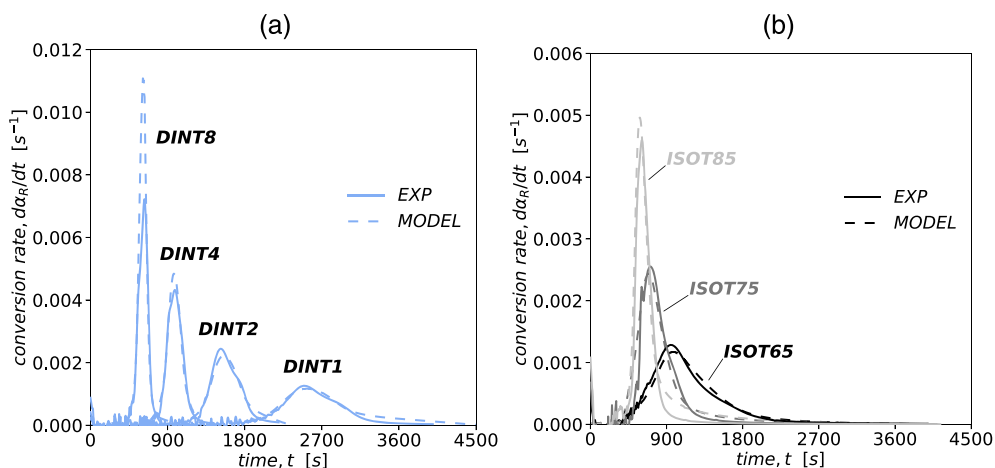

FIGURE 7 Comparison of experimental (continuous lines) and calculated (dashed lines) conversion rates from calorimetric analysis versus time in (a) "dynamic conditions" and (b) "isothermal conditions" [Color figure can be viewed at wileyonlinelibrary.com]
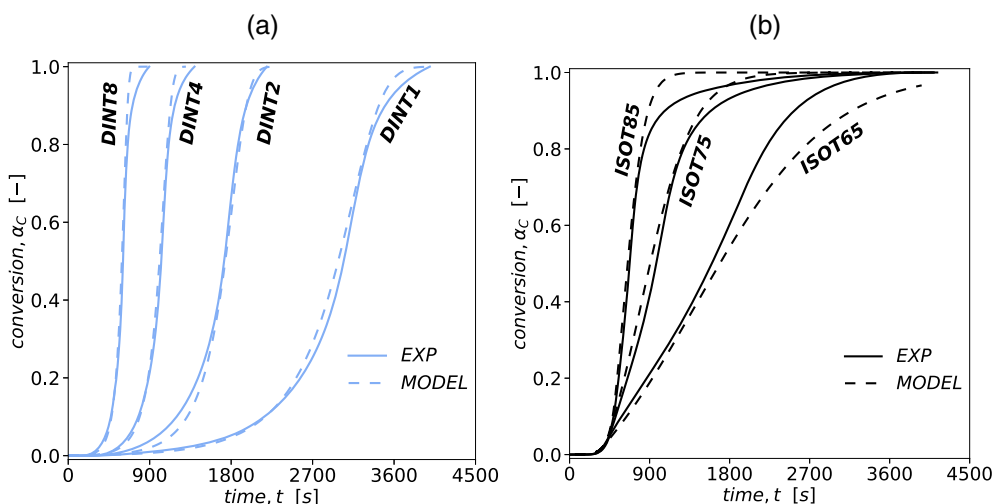

FIGURE 8 Comparison of experimental (continuous lines) and calculated (dashed lines) conversion rates from rheological analysis versus time in (a) "dynamic conditions" and (b) "isothermal conditions" [Color figure can be viewed at wileyonlinelibrary.com]

The deviation observable for $\alpha_C > 0.85$ and $\alpha_R > 0.9$, can be still related to the fact that the mobility of the molecules changes in the final stage of the process, and therefore the kinetics is expected to be different from the modeled one.[16,37] Furthermore, the model ability to predict the DINT8 experiment, which was not considered for the parameters identification, confirms the model validity.

FIGURE 9 Comparison of experimental (continuous lines) and calculated (dashed lines) conversions from calorimetric analysis versus time in (a) "dynamic conditions" and (b) "isothermal conditions" [Color figure can be viewed at wileyonlinelibrary.com]
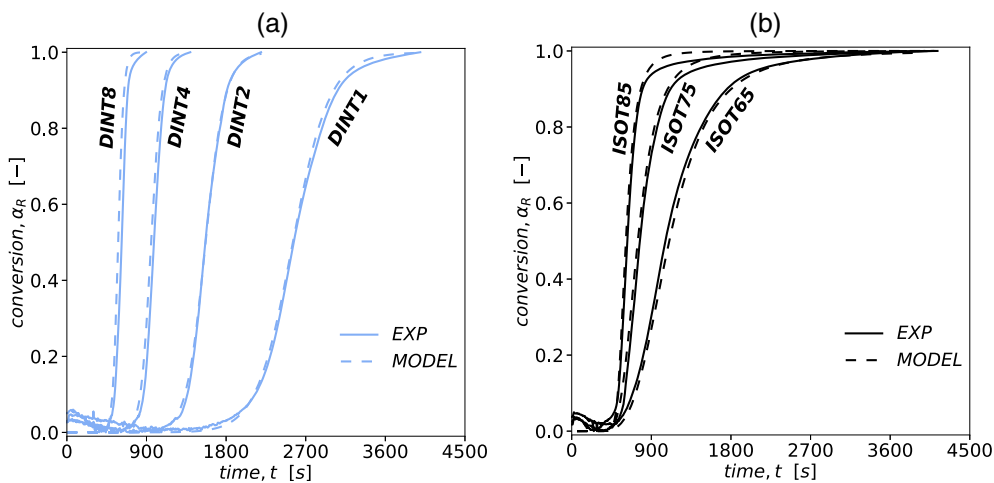
FIGURE 10 Comparison of experimental (continuous lines) and calculated (dashed lines) conversions from rheological analysis versus time in (a) "dynamic conditions" and (b) "isothermal conditions" [Color figure can be viewed at wileyonlinelibrary.com]
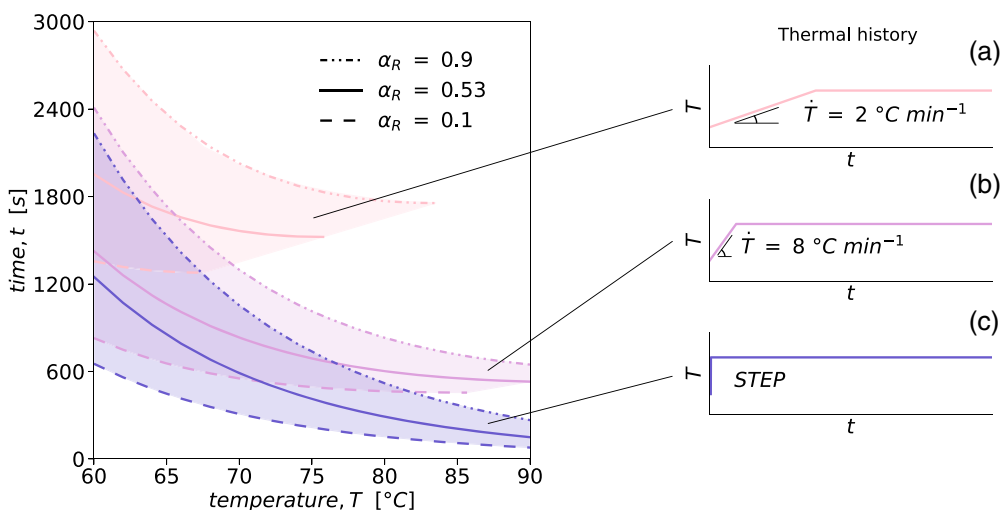
FIGURE 11 Iso-conversion curves map: It allows to evaluate the time required to reach a fixed conversion for a curing process performed under a defined thermal history. The illustrative map refers to isothermal curing conditions differing in the heating ramp: (a) $\dot{T} = 2°C\,min^{-1}$, (b) $\dot{T} = 8°C\,min^{-1}$, (c) ideal step heating. For simplicity, only curves relevant to α_R of 0.1, 0.53 (gel point) and 0.9 are shown [Color figure can be viewed at wileyonlinelibrary.com]

The two models could therefore be used to predict the evolution in time of the crosslinking process for any thermal histories, different from those considered in this study.

The prediction of the kinetics can be very useful for example to predict the processing time, that is, the time until the material has a relatively low viscosity and is thus processable. In particular, the rheological model is the best for this purpose, as it is directly related to mechanical properties.

Iso-conversion curves can be plotted in a time–temperature plot. An example is reported in Figure 11: the map allows to evaluate the time required to reach a defined conversion at a certain temperature for a defined thermal history. The information provided is limited by the time necessary to reach T_c according to the imposed heating ramp.

Figure 11 shows how both the heating rate and the temperature in isothermal curing affect the processability of the material. For example, for an isothermal curing temperature $T_c = 70\,°C$, if the material is instantaneously heated up to T_c (thermal history c in Figure 11), $\alpha_R = 0.1$ is reached in only 5 min and $\alpha_R = 0.53$ (which corresponds to the gel point) is reached in about 10 min. If the heating rate is $\dot{T} = 8\,°C\,min^{-1}$ (thermal history b in Figure 11), it takes about 9 min to reach $\alpha_R = 0.1$ and about 14 min to reach the gel point. If the heating rate is $\dot{T} = 2\,°C\,min^{-1}$, the times are even longer. 26 min are necessary to reach a conversion $\alpha_R = 0.53$ (gel point) and the material reaches $\alpha_R = 0.1$ in about 21 min at a temperature of $67\,°C$ still during heating.

5 | CONCLUSIONS

This work reports on the first systematic investigation of crosslinking reaction of Sylgard184, a PDMS the use of which is widely reported in literature. The investigation was carried out through two methods: the detection of the heat released during the reaction by calorimetric analysis and the measurement of the material dynamic modulus during the network formation by rheological analysis.

The comparison between the results from the two testing methods showed a general agreement as concerns the effect of temperature and heating rate on accelerating the process, but also allowed to emphasize different features of the crosslinking process. Calorimetric and rheometric analyses allowed to highlight different features of the process. A calorimetric characterization clearly shows the initial phases of the chemical reaction, while this detail is not captured by the rheometric observations. On the other hand, rheological analysis, that provides precise information about changes in the material mechanical properties, allows to detect the gel point, which cannot be identified by the calorimetric analysis. The time lag between the time at which the reaction starts and the time at which mechanical properties start to change could be relevant in setting the processing cycle of the material.

The rheological model is expected to be a useful tool for the proper design of the technology for the production of PDMS based product. As a matter of facts, the model allows, on one end, to predict the processing time, and therefore the time available for PDMS molding before crosslinking, and, on the other, to design an appropriate curing cycle for the preparation of the PDMS for a specific application. This last task should also consider the effect of curing conditions on the final structure and resulting properties of the formed PDMS, which is currently under investigation.

ORCID
Tiziana Bardelli https://orcid.org/0000-0001-6156-0026
Claudia Marano https://orcid.org/0000-0002-5319-9610
Francesco Briatico Vangosa https://orcid.org/0000-0002-7088-1064

REFERENCES
[1] G. Koerner, *Silicones, Chemistry and Technology*, CRC Press, Boca Raton **1992**.
[2] F. Schneider, T. Fellner, J. Wilde, U. Wallrabe, *J. Micromech. Microeng.* **2008**, *18*, 065008.
[3] F. Schneider, J. Draheim, R. Kamberger, U. Wallrabe, *Sens. Actuators Phys.* **2009**, *151*, 95.
[4] A. Villanueva, C. Smith, S. Priya, *Bioinspir. Biomim.* **2011**, *6*, 036004.
[5] T. K. Kim, J. K. Kim, O. C. Jeong, *Microelectron. Eng.* **2011**, *88*, 1982.
[6] S.-H. Song, H. Lee, J.-G. Lee, J.-Y. Lee, M. Cho, S.-H. Ahn, *Compos. Part B Eng.* **2016**, *95*, 155.
[7] A. Colombo, H. Zahedmanesh, D. M. Toner, P. A. Cahill, C. Lally, *J. Mech. Behav. Biomed. Mater.* **2010**, *3*, 470.
[8] H.-J. Kim, S.-H. Song, S.-H. Ahn, *Smart Mater. Struct.* **2013**, *22*, 014007.
[9] R. F. Shepherd, F. Ilievski, W. Choi, S. A. Morin, A. A. Stokes, A. D. Mazzeo, X. Chen, M. Wang, G. M. Whitesides, *Proc. Natl. Acad. Sci.* **2011**, *108*, 20400.
[10] W. Wang, J.-Y. Lee, H. Rodrigue, S.-H. Song, W.-S. Chu, S.-H. Ahn, *Bioinspir. Biomim.* **2014**, *9*, 046006.
[11] H. Rodrigue, B. Bhandari, M.-W. Han, S.-H. Ahn, *J. Intell. Mater. Syst. Struct.* **2015**, *26*, 1071.

[12] A. Santiago-Alvarado, A. Cruz-Felix, F. Iturbide, B. Licona-Morán, *Int. J. Eng. Sci. Innov. Technol.* **2014**, *3*, 563.

[13] D. Chang-Yen, R. Eich, B. Gale, *J. Lightwave Technol.* **2005**, *23*, 2088.

[14] J. S. Kee, D. P. Poenar, P. Neužil, L. Yobaş, Y. Chen, *Opt. Express* **2010**, *18*, 21732.

[15] Dow Corning Product information sheet of Sylgard184 **2017**.

[16] S. Vyazovkin, A. K. Burnham, J. M. Criado, L. A. Pérez-Maqueda, C. Popescu, N. Sbirrazzuoli, *Thermochim. Acta* **2011**, *520*, 1.

[17] L. M. Lopez, A. B. Cosgrove, J. P. Hernandez-Ortiz, T. A. Osswald, *Polym. Eng. Sci.* **2007**, *47*, 675.

[18] I.-K. Hong, S. Lee, *J. Ind. Eng. Chem.* **2013**, *19*, 42.

[19] Q. Zhang, B. Song, S. Wang, L. Xu, S. Liu, *Int. Conf. Electron. Packag. Technol.* **2009**, *2009*, 2009.

[20] A. Harkous, G. Colomines, E. Leroy, P. Mousseau, R. Deterre, *React. Funct. Polym.* **2016**, *101*, 20.

[21] J. P. Hernández-Ortiz, T. A. Osswald, *J. Appl. Polym. Sci.* **2011**, *119*, 1864.

[22] F. Wolff, C. Kugler, H. Münstedt, *Rheol. Acta* **2012**, *51*, 71.

[23] M. R. Kamal, S. Sourour, *Polym. Eng. Sci.* **1973**, *13*, 59.

[24] A. C. C. Esteves, J. Brokken-Zijp, J. Laven, H. P. Huinink, N. J. W. Reuvers, M. P. Van, G. de With, *Polymer* **2009**, *50*, 3955.

[25] J. E. Sheats, C. E. Carraher, C. U. Pittman, M. Zeldin, B. M. Culbertson, in *Metal-Containing Polymeric Materials* (Eds: C. U. Pittman, C. E. Carraher, M. Zeldin, J. E. Sheats, B. M. Culbertson), Springer, Boston, MA **1990**.

[26] M. Liu, J. Sun, Q. Chen, *Sens. Actuators Phys.* **2009**, *151*, 42.

[27] P. J. Flory, *Principles of Polymer Chemistry*, Cornell University Press, Ithaca, NY **1953**.

[28] R. J. Young, P. A. Lovell, *Introduction to Polymers*, 3rd ed., CRC Press, Bosa Roca **2011**.

[29] H. J. Borchardt, F. Daniels, *J. Am. Chem. Soc.* **1957**, *79*, 41.

[30] J. C. Domínguez, M. V. Alonso, M. Oliet, E. Rojo, F. Rodríguez, *Thermochim. Acta* **2010**, *498*, 39.

[31] C. W. Macosko, *Rheology: Principles Measurements and Applications*, Wiley-VCH, New York **1994**.

[32] H. H. Winter, F. Chambon, *J. Rheol.* **1986**, *30*, 367.

[33] E. Rudé Payró, J. Llorens Llacuna, *J. Non-Cryst. Solids* **2006**, *352*, 2220.

[34] H. Winter, *Polym. Eng. Sci.* **1698**, *1987*, 27.

[35] C. M. Tung, P. J. Dynes, *J. Appl. Polym. Sci.* **1982**, *27*, 569.

[36] S. Vyazovkin, N. Sbirrazzuoli, *Macromolecules* **1996**, *29*, 1867.

[37] S. Vyazovkin, *New J. Chem.* **2000**, *24*, 913.

[38] H. Stutz, J. Mertes, K. Neubecker, *J. Polym. Sci. Part Polym. Chem.* **1993**, *31*, 1879.